

Mechanics Based Design of Structures and Machines

An International Journal

ISSN: 1539-7734 (Print) 1539-7742 (Online) Journal homepage: <https://www.tandfonline.com/loi/lmbd20>

Mechatronic design, experimental setup, and control architecture design of a novel 4 DoF parallel manipulator

Marina Vallés, Pedro Araujo-Gómez, Vicente Mata, Angel Valera, Miguel Díaz-Rodríguez, Álvaro Page & Nidal M. Farhat

To cite this article: Marina Vallés, Pedro Araujo-Gómez, Vicente Mata, Angel Valera, Miguel Díaz-Rodríguez, Álvaro Page & Nidal M. Farhat (2018) Mechatronic design, experimental setup, and control architecture design of a novel 4 DoF parallel manipulator, Mechanics Based Design of Structures and Machines, 46:4, 425-439, DOI: [10.1080/15397734.2017.1355249](https://doi.org/10.1080/15397734.2017.1355249)

To link to this article: <https://doi.org/10.1080/15397734.2017.1355249>



Published online: 24 Aug 2017.



Submit your article to this journal [↗](#)



Article views: 313



View related articles [↗](#)




View Crossmark data [↗](#)



Citing articles: 8 View citing articles [↗](#)



Mechatronic design, experimental setup, and control architecture design of a novel 4 DoF parallel manipulator

Marina Vallés^a, Pedro Araujo-Gómez^b, Vicente Mata^c, Angel Valera^a , Miguel Díaz-Rodríguez^b, Álvaro Page^d, and Nidal M. Farhat^e

^aInstituto Universitario de Automática e Informática Industrial, Dpto. Ingeniería de Sistemas y Automática, Universitat Politècnica de València, Valencia, Spain; ^bLaboratorio de Mecatrónica y Robótica, Departamento de Tecnología y Diseño, Facultad de Ingeniería, Universidad de los Andes, Mérida, Venezuela; ^cDepartamento de Ingeniería Mecánica y Materiales, Centro de Investigación en Ingeniería Mecánica, Universitat Politècnica de València, Valencia, Spain; ^dInstituto de Biomecánica de Valencia, Universitat Politècnica de València, Valencia, Spain; ^eDepartment of Mechanical and Mechatronics Engineering, Faculty of Engineering and Technology, Birzeit University, Palestine

ABSTRACT

Although parallel manipulators started with the introduction of architectures with six degrees of freedom, a vast number of applications require less than six degrees of freedom. Consequently, scholars have proposed architectures with three and four degrees of freedom, but relatively few four degrees of freedom parallel manipulators have become prototypes, especially of the two rotation and two translation motion types. In this article, we explain the mechatronics design, prototype, and control architecture design of a four degrees of freedom parallel manipulators with two rotation and two translation motions. We chose to design a four degrees of freedom manipulator based on the motion needed to complete the tasks of lower limb rehabilitation. To the author's best knowledge, parallel manipulators between three and six degrees of freedom for rehabilitation of lower limb have not been proposed to date. The developed architecture enhances the three minimum degrees of freedom required by adding a four degrees of freedom, which allows combinations of normal or tangential efforts in the joints, or torque acting on the knee. We put forward the inverse and forward displacement equations, describe the prototype, perform the experimental setup, and develop the hardware and control architecture. The tracking accuracy experiments from the proposed controller show that the manipulator can accomplish the required application.

ARTICLE HISTORY

Received 8 March 2017
Accepted 11 July 2017

KEYWORDS

Control architecture design; kinematics; mechatronics; parallel manipulator; robot control

1. Introduction

From academia to industry, parallel manipulators (PMs) have received a great deal of attention and have become a very active area of research. Examples of PM-based applications can be found as flight and motion simulations (Tsai, 1999), food manipulators (Xu et al., 2008), medical applications (Li and Xu, 2007), milling machines (Pierrot and Company, 1999), assembly manipulators (Chablat and Wenger, 2003), robotic rehabilitation (Vallés et al., 2015), among others.

In terms of the PM architecture, the first of its kind consisted of a based platform connected through six (6) limbs to a mobile platform. The legs arrangement provided six degrees of freedom (DoF) to the end-effector located on the mobile platform (Gough and Whitehall, 1962; Stewart, 1965). This architecture is still applied today to develop new applications, and thus new strategies for designing PM

CONTACT Angel Valera  giuprog@isa.upv.es  Instituto Universitario de Automática e Informática Industrial, Universitat Politècnica de València, Camino de Vera, s/n, 46022, Valencia, Spain.

Color versions of one or more of the figures in the article can be found online at www.tandfonline.com/lmbd.

Communicated by Ashitava Ghosal.

is a topic of continuous research (Cao et al., 2015). However, since many applications require less than six DoF, new architectures with less DoF called limited DOF PM have been developed. One advantage of designing limited DoF PM is that they maintain some advantages of six DoF while reducing development cost (designing, manufacturing, and operation). Examples of this kind of PM are the delta robot with three translational DoF (Clavel, 1988) and 3-RPS (Lee and Arjunan, 1992), (Carretero et al., 2000). There is also 3-PRS with two rotational (2R) motions and one translational (1T) DoF (Chablat and Wenger, 2003; Vallés et al., 2012), where R, P, and S stand for the revolute, prismatic, and spherical joints, respectively. Some scholars have proposed a subset of platforms with four DoF, mainly for flight simulation purpose, and with three rotational and one translation DOF (3R1T parallel manipulators). Nevertheless, the literature regarding four DoF PMs is limited compared with the series of six, three, and two DoF (Zarkandi, 2011). More recently, Gan et al. (2015) proposed a 2RPS–2UPS architecture to deal with automating fiber placement for aerospace part manufacturing. Among the four DoF (without actuation redundancy), we found in the literature that very few of them have become actual prototypes, and in the field of rehabilitation, we found that a reconfigurable manipulator with four DoF was built (Yoon et al., 2006).

Nowadays, PM are emerging as a conceptual design in the field of rehabilitation robotics (Cazalilla et al., 2016). In the field of lower limb rehabilitation (LLR), most of the PMs developed to date consist of two and three rotational DoF, mainly because they focus on ankle rehabilitation (Jamwal et al., 2015). Girone et al. (2001) proposed a six DoF as an LLR, although the authors basically adapted a Gough PM architecture for the required task. The above architectures can be suitable for very restricted motions such as the one which takes place in ankle rehabilitation. However, they cannot be extended to rehabilitation of other joints such as the knee or hip. These joints require flexion–extension motion in the sagittal plane as well as small rotations involving systems with three or more DoF, of which at least two must be translational motion. A six DOF PM can be seen as a first design concept for LLR (Rastegarpanah et al., 2016). As we mentioned before, this solution increases cost and requires an intricate control and dynamic robot model (Jamwal et al., 2015). We are interested in developing a relatively simpler solution.

To look for a simpler solution, we need to establish the essential motion which takes place in the LLR. In this regard, the task requires at least three DoF, i.e., two translations for planar motion and one rotation for flexion–extension motion (Araujo-Gómez et al., 2016; Mohan et al., 2017). To the authors' best knowledge, we have not found PMs for LLR between three and six DoF. We have found serial manipulators which are exoskeleton-based, allowing motions that are compatible with lower limb joint motions (Díaz et al., 2011). Conversely, exoskeleton is unable to deal with combinations of normal or tangential efforts in the joint, or torque acting on the knee, which limits the ability to portray some of the rehabilitation and diagnosis tasks for the knee joint. For instance, wall squats, decline eccentric squats, exercises that involve applying a relevant force in the anteroposterior, or the ability to control the torque applied to the knee (Escamilla et al., 2012).

In this article, we present the mechatronic design of a two translational and 2R four DoF PMs, which is able to perform a large number of procedures applicable to LLR, where the mobile platform can simulate the foot trajectory during physiotherapy exercises. We also present the experimental setup including the control architecture design. The main contributions of our article are the following: (1) the developed architecture enhances the three minimum DoF required by adding four DoF, which allows combinations of normal or tangential efforts in the joint, or torque acting on the knee. (2) The robot is able to apply torque to the ligaments of the knee joint without parasite motion on the end-effector. (3) Although many published papers deal with four DoF and present the kinematics and dynamics analysis, few prototypes have been built and few have provided its experimental setup.

2. Parallel manipulator design

2.1. Presentation of the four DoF parallel manipulator

We have taken the following guidelines into account when designing the manipulator:

- The manipulator should bear a ratio of the person's weight. In addition, the device should be portable and its size as small as possible. As a design concept, a PM meets the specification.
- One of the legs of the PM should be located in the center of mobile platform to bring both stability and load capacity to the manipulator.
- The end-effector should be able to move with planar motion on the plane defined by the axis which is normal to the sagittal plane. In addition, it should have two rotations, one parallel to the y -axis and the second one which is normal to the moving platform. An RPU central leg constrains the end-effector to move in a plane (sagittal plane), the U joint defines the rotational DoF.
- The four DoF can be achieved with four legs (Merlet, 2006). Therefore, the manipulator should have three additional legs. Since the central leg constrains the end-effector to the required DoF, the external legs should allow six DoF. A UPS leg is considered.
- The spherical (S) and the universal (U) joints located on the mobile platform should lie in the same plane, thus avoiding or reducing parasite motions on the end-effector.

Figure 1 shows the 3UPS + RPU, which consists of four legs equipped with an active prismatic joint (P). Figure 2 shows the actual PM and its schematic representation. The legs are located as follows: three identical 3-UPS external limbs (U stands for universal joint, the underlying letter P indicates the actuated joint), and a central RPU limb. The external limbs are equally spaced around the central limb at a radius r in the case of fixed base and a radius r_m for the mobile platform (Fig. 2).

Figure 2 also shows the arrangement of kinematic pairs. The first axis of rotation of the U-joints, located at the base, points parallel to the axis of the central R joint. In the same figure, the reference

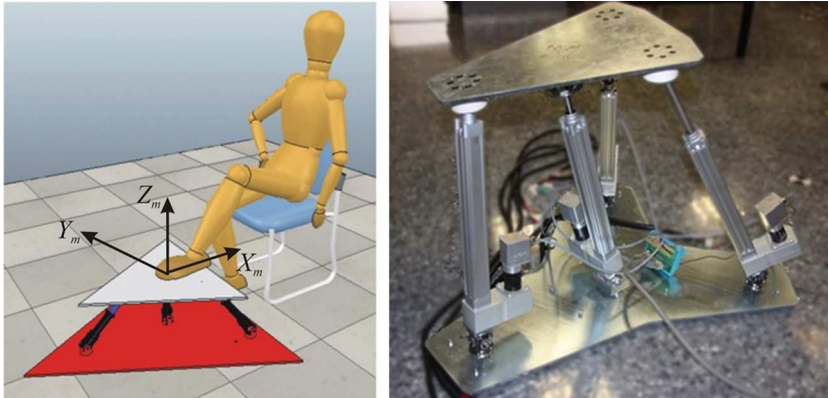


Figure 1. Virtual and actual four DoF parallel manipulator. Note: DoF, degrees of freedom.

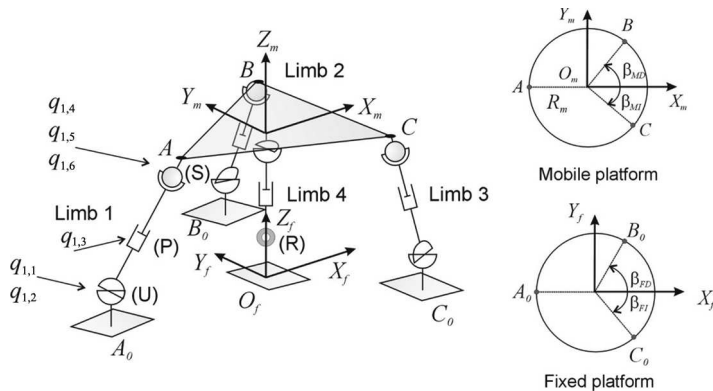


Figure 2. Actual PM and localization of the coordinate systems. Note: PM, parallel manipulator.

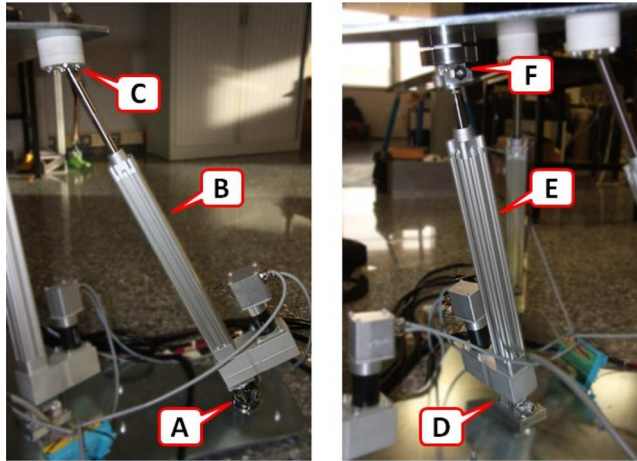


Figure 3. Detailed parts of the actual PM. Note: PM, parallel manipulator.

systems attached both to the fixed base and to the mobile platform are also depicted. The proposed PM is made up of nine mobile links, five type I kinematic joints (four prismatic + one rotational), four type II kinematic joints (universal), and three type III kinematic joints (spherical). Following the Grübler Kutzbach criterion, the PM has four DoF.

Figure 3 shows the actual PM in more detail. Each external limb consists of: (A) a universal joint connecting the fixed platform to the limb, (B) a prismatic joint actuated by the DC motor, and (C) a spherical passive joint connecting the limb to the mobile platform. The central limb consists of: (D) a passive revolute joint connecting the fixed platform to the limb, (E) a prismatic joint controlled by the DC motor, and (F) a universal passive joint connecting the limb to the mobile platform.

Table 1 shows the D–H parameters for the external legs of the actual parallel kinematics mechanism (PKM). The subscripts i, j denote the joint j on limb i . Figure 2 shows the parameters corresponding to leg 1. Table 2 shows the D–H parameters for the central leg. In both cases, we use Paul’s notation (Paul, 1981).

2.2. Four DoF parallel manipulator inverse kinematics

Given the rotational (pitch (β) and yaw (ψ)) angles, and the translations in the X_f - Z_f plane, the inverse position equations consist of finding the linear displacement of the actuators: $q_{i,3}; i = 1, \dots, 3$, for the

Table 1. D–H parameter for the UPS limbs (for $i = 1, \dots, 3$) of the four DoF PM.

j	α_{ij}	a_{ij}	d_{ij}	θ_{ij}
1	$-\pi/2$	0	0	$q_{i,1}$
2	$\pi/2$	0	0	$q_{i,2}$
3	0	0	$q_{i,3}$	0
4	$\pi/2$	0	0	$q_{i,4}$
5	$\pi/2$	0	0	$q_{i,5}$
6	$\pi/2$	0	0	$q_{i,6}$

DoF PM, degrees of freedom parallel manipulators.

Table 2. D–H Parameter for the RPS limb of the four DoF PM.

j	α_{ij}	a_{ij}	d_{ij}	θ_{ij}
1	$-\pi/2$	0	0	$q_{4,1}$
2	$\pi/2$	0	0	π
3	$\pi/2$	0	$q_{4,2}$	$q_{4,3}$
4	0	0	0	$q_{4,4}$

DoF PM, degrees of freedom parallel manipulators.

external limbs (UPS) and $q_{4,2}$ for the central limb (RPU). This problem will be divided into two parts: first, we obtain the UPS limb coordinates $q_{i,1}, q_{i,2}, q_{i,3}, i = 1 \dots 3$ and the central RPU limb coordinates $q_{4,1}, q_{4,2}$. Second, we obtain the passive coordinates ($q_{i,4}, q_{i,5}, q_{i,6}, i = 1 \dots 3$) of the UPS limbs and $q_{4,3}$ and $q_{4,4}$ of RPU.

To define the orientation and translation of frame j with regard to $j - 1$ for the i -th limb, the following transformation matrix can be used:

$${}^{j-1}H_j^i = \begin{bmatrix} C_{\theta_{ij}} & -C_{\alpha_{ij}} \cdot S_{\theta_{ij}} & S_{\alpha_{ij}} \cdot S_{\theta_{ij}} & a_{ij} \cdot C_{\theta_{ij}} \\ S_{\theta_{ij}} & C_{\alpha_{ij}} \cdot C_{\theta_{ij}} & -S_{\alpha_{ij}} \cdot C_{\theta_{ij}} & a_{ij} \cdot S_{\theta_{ij}} \\ 0 & S_{\alpha_{ij}} & C_{\alpha_{ij}} & d_{ij} \\ 0 & 0 & 0 & 1 \end{bmatrix}, \quad (1)$$

where S and C stand for sine and cosine of the corresponding angle. The closure equation for the central limb can be written as follows:

$$\begin{bmatrix} x_m \\ y_m \\ z_m \end{bmatrix} = \left[{}^fH_0^4 \cdot {}^0H_1^4(q_{4,1}) \cdot {}^1H_2^4(q_{4,2}) \right]_{\substack{4,1 \\ 4,2 \\ 4,3}} \quad (2)$$

for the other limbs, the closure equations can be established as follows:

$$\begin{bmatrix} x_m \\ y_m \\ z_m \end{bmatrix} + {}^fR_m \cdot \begin{bmatrix} -r_m \\ 0 \\ 0 \end{bmatrix} = \left[{}^fH_0^1 \cdot {}^0H_1^1(q_{1,1}) \cdot {}^1H_2^1(q_{1,2}) \cdot {}^2H_3^1(q_{1,3}) \right]_{\substack{4,1 \\ 4,2 \\ 4,3}}$$

$$\begin{bmatrix} x_m \\ y_m \\ z_m \end{bmatrix} + {}^fR_m \cdot \begin{bmatrix} r_m \cdot \cos(\beta_m) \\ r_m \cdot \sin(\beta_m) \\ 0 \end{bmatrix} = \left[{}^fH_0^2 \cdot {}^0H_1^2(q_{2,1}) \cdot {}^1H_2^2(q_{2,2}) \cdot {}^2H_3^2(q_{2,3}) \right]_{\substack{4,1 \\ 4,2 \\ 4,3}} \quad (3)$$

$$\begin{bmatrix} x_m \\ y_m \\ z_m \end{bmatrix} + {}^fR_m \cdot \begin{bmatrix} r_m \cdot \cos(\beta_m) \\ -r_m \cdot \sin(\beta_m) \\ 0 \end{bmatrix} = \left[{}^fH_0^3 \cdot {}^0H_1^3(q_{3,1}) \cdot {}^1H_2^3(q_{3,2}) \cdot {}^2H_3^3(q_{3,3}) \right]_{\substack{4,1 \\ 4,2 \\ 4,3}}$$

for points A , B , and C , respectively. fR_m is the rotation matrix of the mobile platform with respect to the fixed reference systems $\{O_f - X_f Y_f Z_f\}$. Subscript $[4, 1 \dots 3]$ indicates that only the fourth column from rows 1 to 3 of the matrix is considered.

Equation (2) applied to the central limb,

$$\begin{aligned} x_m &= -\sin(q_{4,1}) \cdot q_{4,2} \\ y_m &= 0 \\ z_m &= \cos(q_{4,1}) \cdot q_{4,2} \end{aligned} \quad (4)$$

From these equations, we can easily obtain the active generalized coordinate $q_{4,2}$ and also the passive one, $q_{4,1}$. For the external limbs, a similar procedure can be followed to obtain explicit expressions for the generalized coordinates. For instance, in the case of limb 1, the active generalized coordinate and the first two passive coordinates can be obtained as follows:

$$\begin{aligned} a &= x_m^2 + z_m^2 + r^2 + r_m^2 + 2 \cdot r \cdot x_m + 2 \cdot r_m \cdot z_m \cdot \text{sen}(\theta) - 2 \cdot r_m \cdot x_m \cdot \cos(\theta) \cdot \cos(\psi) \\ &\quad - 2 \cdot r \cdot r_m \cdot \cos(\theta) \cdot \cos(\psi) \end{aligned}$$

$$b = -x_m^2 - z_m^2 - r^2 - r_m^2 - 2 \cdot r \cdot x_m - 2 \cdot r_m \cdot z_m \cdot \text{sen}(\theta) + 2 \cdot r \cdot r_m \cdot \text{cos}(\theta) \cdot \text{cos}(\psi) + 2 \cdot r_m \cdot x_m \cdot \text{cos}(\theta) \cdot \text{cos}(\psi) + r_m^2 \cdot \text{cos}^2(\theta) \cdot \text{sen}^2(\psi)$$

$$q_{1,3} = \sqrt{a} \tag{5}$$

$$q_{1,2} = \text{atan2} \left(\sqrt{\frac{b}{a}}, \frac{r_m \cdot \text{cos}(\theta) \cdot \text{sen}(\psi)}{\sqrt{-b}} \right) \tag{6}$$

$$q_{1,1} = \text{atan2} \left(\frac{z_m + r_m \cdot \text{cos}(\theta)}{\sqrt{-b}}, \frac{r_m \cdot \text{cos}(\theta) \cdot \text{sen}(\psi)}{\sqrt{-b}} \right) \tag{7}$$

for the second stage, the remaining passive generalized coordinates, $q_{i,4}, q_{i,5}, q_{i,6}$, of the external limbs can be obtained from the equation as follows:

$${}^fR_3(q_{i,1}, q_{i,2}, q_{i,3}) \cdot {}^3R_6(q_{i,4}, q_{i,5}, q_{i,6}) = {}^fR_m(\varphi, \theta, \psi) \quad i = 1 \dots 3. \tag{8}$$

2.3. Four DoF parallel robot forward displacement

For each of the robot's legs, the following vector closure equations can be established (Fig. 4).

$$\begin{aligned} \vec{r}_{A_0A}(q_{1,1}, q_{1,2}, q_{1,3}) &= \begin{bmatrix} x_m \\ 0 \\ z_m \end{bmatrix} + {}^fR_m(\theta, \psi) \cdot \begin{bmatrix} -r \\ 0 \\ 0 \end{bmatrix} \\ \vec{r}_{B_0B}(q_{2,1}, q_{2,2}, q_{2,3}) &= \begin{bmatrix} x_m \\ 0 \\ z_m \end{bmatrix} + {}^fR_m(\theta, \psi) \cdot \begin{bmatrix} r \cdot \text{cos}(\beta_{MD}) \\ r \cdot \text{sen}(\beta_{MD}) \\ 0 \end{bmatrix} \\ \vec{r}_{C_0C}(q_{3,1}, q_{3,2}, q_{3,3}) &= \begin{bmatrix} x_m \\ 0 \\ z_m \end{bmatrix} + {}^fR_m(\theta, \psi) \cdot \begin{bmatrix} r \cdot \text{cos}(\beta_{MI}) \\ -r \cdot \text{sen}(\beta_{MI}) \\ 0 \end{bmatrix} \\ \vec{r}_{O_fO_m}(q_{4,1}, q_{4,2}) &= \begin{bmatrix} x_m \\ 0 \\ z_m \end{bmatrix} \end{aligned} \tag{9}$$

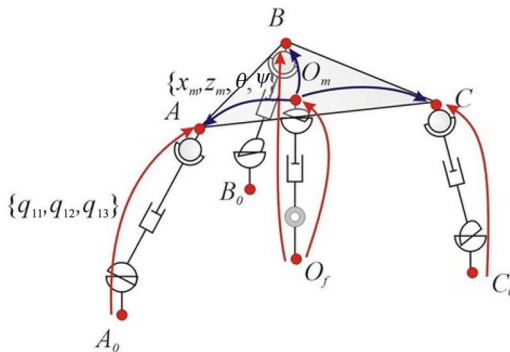


Figure 4. Close-loops of the manipulator.

From Eq. (9), a system of 11 nontrivial equations with 11 unknowns can be obtained. This system could be solved by the Newton–Raphson (N-R) numerical algorithm. However, to improve the calculation time and the convergence speed, the passive generalized coordinates will be eliminated from those equations, leading to a system of only four equations,

$$\begin{aligned}\Phi_1 = & q_{1,3}^2 - r^2 - 2 \cdot r \cdot x_m + 2 \cdot r \cdot r_m \cdot \cos(\psi) \cdot \cos(\theta) - x_m^2 \\ & + 2 \cdot x_m \cdot r_m \cdot \cos(\psi) \cdot \cos(\theta) - z_m^2 - 2 \cdot z_m \cdot r_m \cdot \sin(\theta) - r_m^2 = 0\end{aligned}\quad (10)$$

$$\begin{aligned}\Phi_2 = & q_{2,3}^2 - r^2 + 2 \cdot r \cdot r_m \cdot \sin(\beta_{FD}) \cdot \cos(\beta_{MD}) \cdot \sin(\psi) \cdot \cos(\theta) \\ & + 2 \cdot r \cdot r_m \cdot \sin(\beta_{FD}) \cdot \sin(\beta_{MD}) \cdot \cos(\psi) + 2 \cdot r \cdot x_m \cdot \cos(\beta_{FD}) \\ & + 2 \cdot r \cdot r_m \cdot \cos(\beta_{FD}) \cdot \cos(\beta_{MD}) \cdot \cos(\psi) \cdot \cos(\theta) \\ & - 2 \cdot r \cdot r_m \cdot \cos(\beta_{FD}) \cdot \sin(\beta_{MD}) \cdot \sin(\psi) - x_m^2 \\ & - 2 \cdot x_m \cdot r_m \cdot \cos(\beta_{FD}) \cdot \cos(\psi) \cdot \cos(\theta) + 2 \cdot x_m \cdot r_m \cdot \sin(\beta_{MD}) \cdot \sin(\psi) \\ & - r_m^2 - z_m^2 + 2 \cdot z_m \cdot r_m \cdot \cos(\beta_{MD}) \cdot \sin(\theta) = 0\end{aligned}\quad (11)$$

$$\begin{aligned}\Phi_3 = & q_{3,3}^2 - r^2 - r_m^2 + 2 \cdot r \cdot r_m \cdot \cos(\beta_{FI}) \cdot \cos(\beta_{MI}) \cdot \cos(\psi) \cdot \cos(\theta) \\ & + 2 \cdot z_m \cdot r_m \cdot \cos(\beta_{MI}) \cdot \sin(\theta) + 2 \cdot r \cdot x_m \cdot \cos(\beta_{FI}) - 2 \cdot x_m \cdot r_m \cdot \sin(\beta_{MI}) \cdot \sin(\psi) \\ & - 2 \cdot r \cdot r_m \cdot \sin(\beta_{FI}) \cdot \cos(\beta_{MI}) \cdot \sin(\psi) \cdot \cos(\theta) - z_m^2 \\ & + 2 \cdot r \cdot r_m \cdot \cos(\beta_{FI}) \cdot \sin(\beta_{MI}) \cdot \sin(\psi) - x_m^2 \\ & - 2 \cdot x_m \cdot r_m \cdot \cos(\beta_{MI}) \cdot \cos(\psi) \cdot \cos(\theta) + 2 \cdot r \cdot r_m \cdot \sin(\beta_{FI}) \cdot \sin(\beta_{MI}) \cdot \cos(\psi) = 0\end{aligned}\quad (12)$$

$$\Phi_4 = q_{4,3}^2 - x_m^2 - z_m^2 = 0. \quad (13)$$

The N-R algorithm enables each set of active generalized coordinates of Eqs. (10)–(13) to be solved faster than the 11 coordinate system represented in Eq. (9). To avoid singular configurations, an asymmetrical array of the legs is proposed. Through a process of trial and error and considering the range of motion for LLR, the following values were selected for the geometric parameters of the PM: $r = 0.400$ mm, $r_m = 0.200$ mm, $\beta_{FD} = 50^\circ$, $\beta_{FI} = 40^\circ$, $\beta_{MD} = 40^\circ$, and $\beta_{MI} = 30^\circ$.

3. Mechatronic manipulator development

Four DC motors equipped with power amplifiers have been used to actuate the four DoF PM. The actuators are *Maxon RE40 Graphite Brushes 150 W* motors. These high-quality motors are fitted with powerful permanent magnets and an ironless rotor as well as being compact, powerful, low-inertia 150 W motors. The performance specifications of these *Maxon's* motors are 24 V nominal voltage, 6940 rpm nominal speed, 6 A max. continuous current, and 2420 mNm stall torque. The characteristics of the motor match the actuation requirement.

These actuators are equipped with encoder sensors and brakes. The encoder sensor is the *ENC DEDL 9149* system which is a digital incremental encoder with 500 pulses per revolution, three channels and 100 kHz max. operating frequency. The brake system is the *Brake AB 28 system*, which is a 24 V, 0.4 Nm permanent-magnet, single-face brake for DC motors that prevent rotation of the shaft at standstill or when the motor power is turned off.

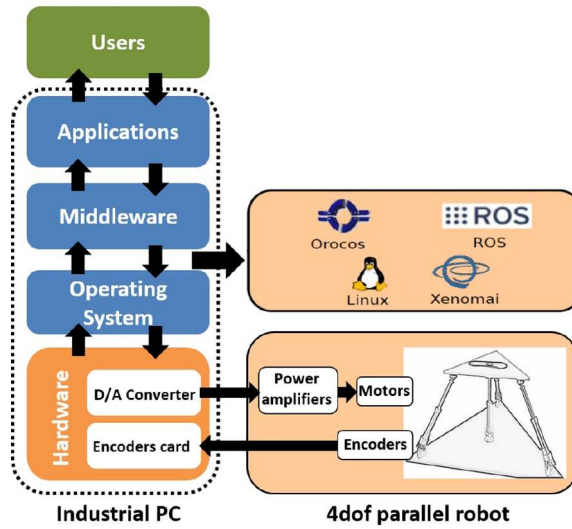


Figure 5. Manipulator control architecture. Note: DoF, degrees of freedom; ROS, robot operating system.

3.1. Hardware control architecture

An industrial PC and a power amplifier stage have been used to implement the control architecture for this PM (Fig. 5). The PC is based on a high performance 4U Rackmount industrial system with seven PCI slots and seven ISA slots. It has a 3.10 GHz Intel® CORE i7 processor and 4 GB DDR3 1333 MHz SDRAM. The industrial PC is equipped with two *Advantech*TM data acquisition cards: *PCI-1720* and *PCI-1784*. The *PCI-1720* card has been used to supply the control actions for each parallel robot actuator, providing four 12-bit isolated digital-to-analog outputs for the Universal PCI 2.2 bus. The card has multiple output ranges (0~5 V, 0~10 V, ± 5 V, ± 10 V), a programmable software and 2500 V DC isolation protection between the outputs and the PCI bus. The *PCI-1784* card is a four-axis quadrature encoder and counter add-on card for the PCI bus. The card includes four 32-bit quadruple AB phase encoder counters, an onboard 8-bit timer with a wide range time-based selector and it is optically isolated up to 2500 V.

An amplifier unit has been developed to control the Maxon's motors. It consists of three stages: an analog to pulse width modulation (PWM) stage, an H-bridge gate driver, and a field-effect transistor (FET) stage (Fig. 6). The first stage transforms the analog voltage supplied by the PC control into a PWM. The analog to PWM stage is based on an *LTC6992* silicon oscillator (*TimerBlox*[®]). The output frequency is determined by a single resistor that programs the *LTC69920*'s internal master oscillator frequency.

The PWM signal and the movement sense (provided by a digital output from the PC control) are supplied to the H-bridge gate driver, which is based on the *DRV8701* device from *Texas Instruments*[®] with

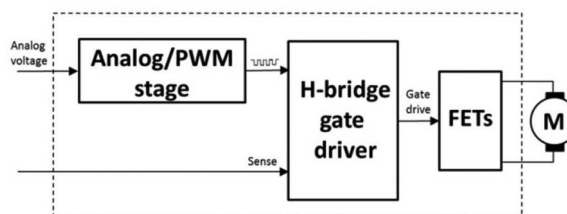


Figure 6. Power amplifier stage. Note: PWM, pulse width modulation.

a brushed DC motor full-bridge driver that uses four external N-channel Metal-oxide-semiconductor Field-effect transistor (MOSFETs) targeted to drive a 12 to 24 V bidirectional brushed DC motor.

Finally, the power amplifier unit has four MOSFETs in a full H-bridge configuration.

3.2. Software control architecture

The software architecture represents one of the critical aspects when implementing a new robot system. In recent years, there has been an increase in component-based software development due to the following advantages:

- Modular design and structure.
- Fully reusable code and modules.
- Reconfigurable modules.
- Distributed execution of the modules, improving total execution time.

Since different control schemes share common parts, the modular design consists of developing each part as a module, thus ending up with several modules. The developer then uses these modules to implement different controllers as if building a puzzle. The developer can configure (making connections between modules) and run the control scheme by inserting the necessary modules. Note that, although developing the modules can be a complicated task at first, the component-based software makes the programmer's job easier in the long run because if a module works correctly in one particular scheme, it will certainly work as well in another control scheme. In addition to the advantages discussed above, this approach minimizes the chance of programming errors in the implementation of any of the modules.

The control architecture (Fig. 5) uses an industrial PC with Linux Ubuntu 12.04 operating system. The rehabilitation therapy requires that the control scheme is able to be run real time, which can be obtained by the real-time kernel patch Xenomai. The proposed control architecture presents two main advantages: (1) the architecture allows us to eventually implement and program any required control algorithm as well as allowing us to use external sensors, such as artificial vision, cameras, force sensors, and accelerometers by only plugging the appropriate module. (2) Since the programming platform was built with free software tools, the control architecture is low cost, including the cost of an industrial PC equipped with industrial data acquisition cards, the cost remains below \$2000.

The robot control algorithms are developed by taking advantage of the middleware *open robot control software* (Orocos (Bruyninckx et al., 2002)) and *robot operating system* (ROS (Garage, 2009)). Nowadays, Orocos represents one of the best real-time motion control frameworks available, but it does have certain constraints when trying to achieve something other than control itself. One of the solutions is ROS, which was designed as a conglomeration of various tools organized in packages. Each package (or "stack") may contain libraries, executables, or scripts and a manifest which defines the dependencies on other packages and meta-information about the package itself. A ROS package called *rtt ros integration* allows Orocos components to connect to the ROS network making both middleware fully compatible.

Concisely, ROS provides many tools and functionalities which are useful when developing robotic applications, while Orocos provides a solid core for real-time control. Both types of software complement each other and widen the range of applications they can offer as standalone platforms.

4. Control of the four DoF PM

The control of the PM can be developed through different control strategies. For instance, model-based controllers which compensate for the nonlinearities of the robot (such as inertial, gravitational, and Coriolis terms) by adding these dynamic terms to the control action. These kinds of controllers have two main problems. First, they are more difficult to program and have greater computational complexity. Second, model-based controllers require the model dynamic parameters, and therefore a parameter identification process is needed (Díaz-Rodríguez et al., 2010).

In this article, a passivity-based controller has been developed to control the novel four DoF PM. The passivity-based approach solves the control problem by taking advantage of the passivity property of the

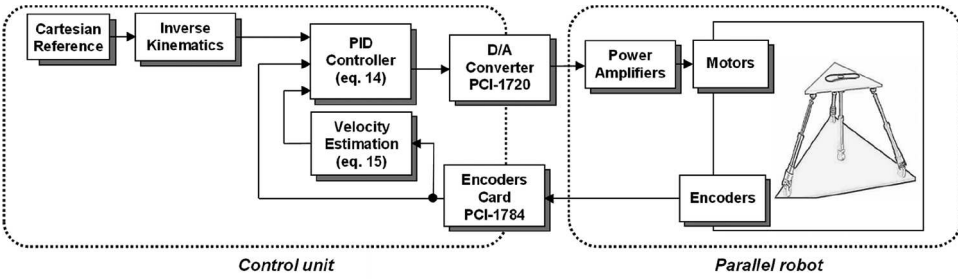


Figure 7. Passivity-based controller implementation in the open control architecture.

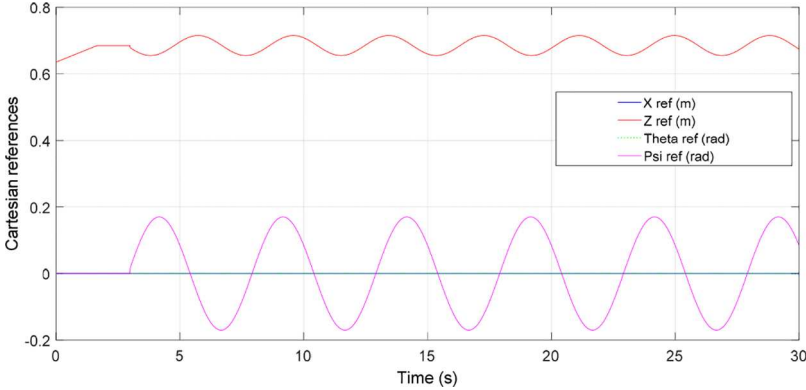


Figure 8. Cartesian reference for the first movement of the robot.

Table 3. Mean errors (m).

	Joint 13	Joint 23	Joint 33	Joint 42
First movement	-4.570e-5	-2.0528e-5	-2.8629e-5	4.3646e-5
Second movement	-8.961e-5	-4.6443e-5	-1.082e-4	3.343e-4

robot system’s physical structure by reshaping the natural energy of the system in such a way that the tracking control objective is achieved (Ortega and Spong, 1989).

The control algorithm is based on the work of Ortega et al. (2013). The control law obeys the following equation:

$$\tau_c = -K_p \cdot e - K_d \cdot v - K_i \cdot \int_0^t (e + v) dt, \tag{14}$$

where $K_p, K_d,$ and K_i are positive definite diagonal matrices. The controller which offers significant system performance and robustness properties is PID. This controller has proportional, derivative, and integral components. The first calculates the error between the active generalized coordinates and their references ($e = q - q_d$). The active coordinate values of the linear actuators are measured using the encoder card. The derivative component depends on the velocity of the joints, and because the proposed robot does not provide velocity sensors, the velocity measurement for this controller has been replaced by approximate differentiation:

$$v = \text{diag} \left\{ \frac{b_i s}{s + a_i} \right\} \cdot q \tag{15}$$

with $a_i > 0$ and $b_i > 0$. Finally, the controller provides an integral component which is introduced in the control law as a standard practical remedy to compensate for the robot gravity term.

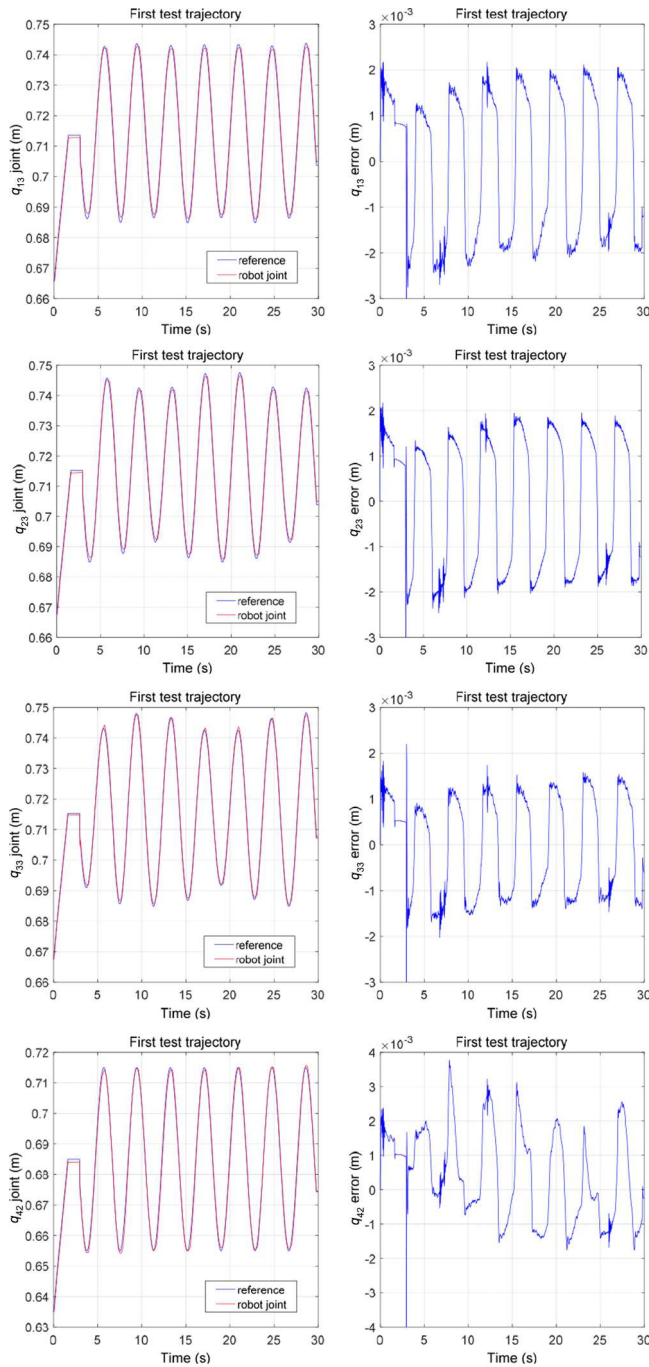


Figure 9. Active robot coordinates and position errors.

This control algorithm has been developed in the open control architecture using the programmed Orocos/ROS modules (Fig. 7). The *Cartesian reference* module calculates the movement references in the Cartesian plane, and the *inverse kinematics* module obtains the references for the four active joints of the robot coordinates (q_{13_ref} , q_{23_ref} , q_{33_ref} , and q_{24_ref}). The robot coordinates are obtained by the *encoders*

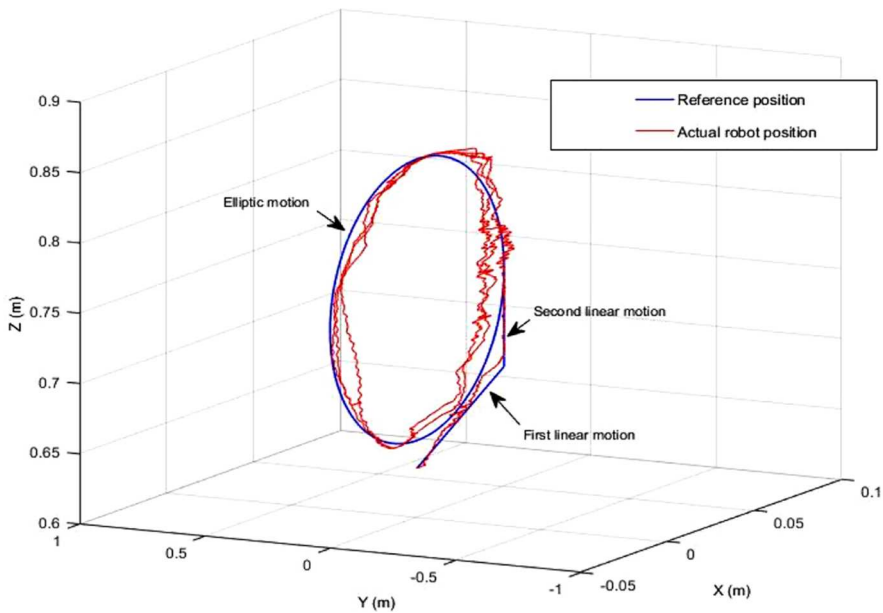


Figure 10. Cartesian reference and actual robot position for the second trajectory.

card PCL-1784 module. The *velocity estimation* module provides the robot velocity estimation following the Eq. (15). The *PID controller* module calculates the control action depending on the proportional, derivative, and integral terms, which it then provides to the actuator module which is in turn responsible for performing digital-analog conversions through the Advantech PCI-1720 card.

To validate the robot design and control architecture, several trajectories have been tested. Due to the space limit, only two of them are included in the article. Figure 8 shows the references for a first execution. In this case, the reference for the Z coordinate and the yaw orientation is based on a sinusoidal motion. The references for the X coordinate and the pitch orientation remain motionless.

Figure 9 presents the response of four active coordinates of the parallel manipulator, according to the Cartesian references proposed above. The first column of this figure shows the joint references (obtained by the inverse kinematics of the robot using Eqs. (5)–(8)) and the robot joint positions. The second column shows the position error. As we can clearly see, the manipulator follows the required trajectory with very small mean errors (Table 3). In addition, the phase offset has been calculated according to Ramsay and Silverman (1997), where the value is very low (41.5 ± 7.0 ms) and shows that the controller presents a very fast response which, in all cases, is lower than the human time reaction (more than 150.0 ms).

Figure 10 shows (in blue) the references for a second execution. In this case, the reference is an elliptic motion in the X – Z plane. Before the periodic motion, the center of the mobile platform follows a linear motion path from the origin (0, 0, 0.635) to the positions (0.05, 0, 0.69), and then a second movement on the Z -axis to the points (0.05, 0, 0.75). The actual robot response is represented in black.

Figure 11 presents the response of the four active coordinates of the parallel manipulator for the second trajectory test. This figure shows the joint references and the robot joint positions as well as the control action applied. As in the first test trajectory, the manipulator response accomplishes the task.

Table 3 shows the difference in the reference value and the actual PM active joints for the two movements presented in Figs. 8 and 10. This difference is described by the mean error value. As shown in this table, the control algorithm implemented gives a very low error, which means that the system achieves the specified reference without any problems.

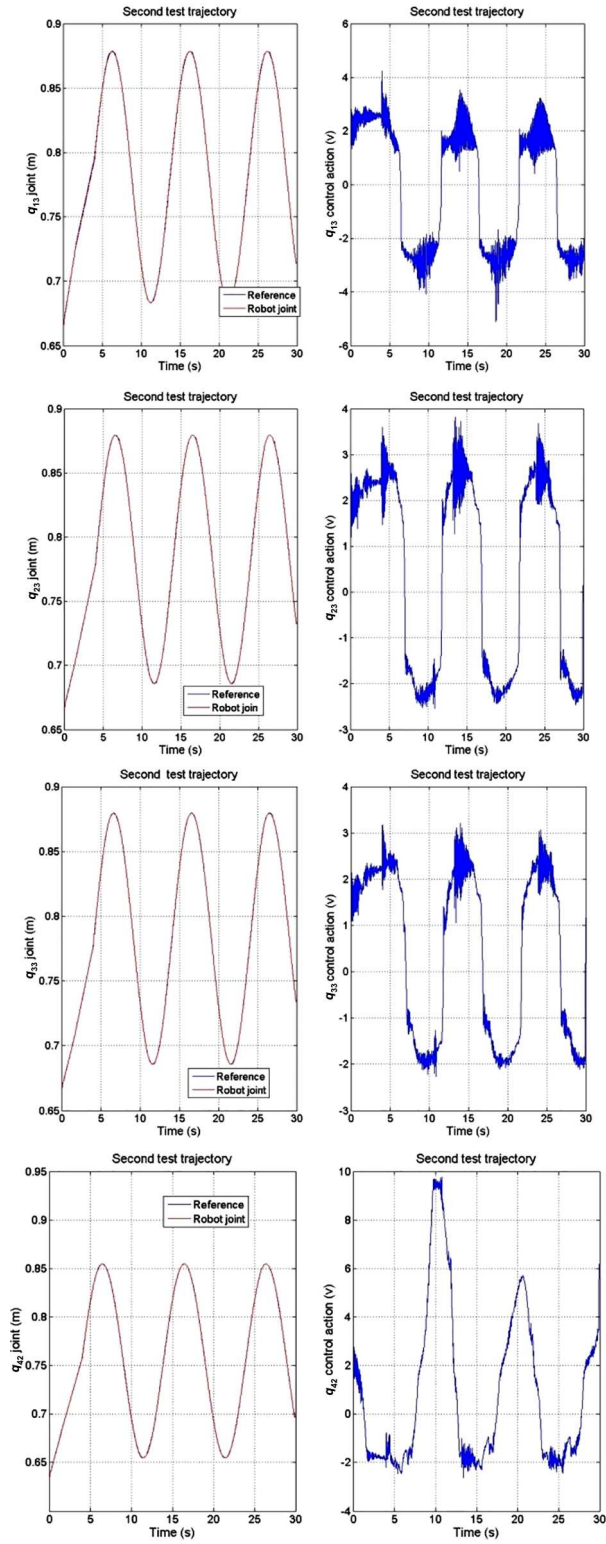


Figure 11. Active robot coordinates and control actions.

5. Conclusion

This article has shown the development of a novel low-cost four DoF parallel manipulator. The PM design was based on the need to develop a LLR system. The developed manipulator allows us to apply combinations of normal or tangential efforts in the leg joints as well as torque acting on the knee which, to the authors' best knowledge, enhances previous designs. We have fully developed the mechatronic design, mechanical structure, electromechanical actuators, and control system. In this regard, we have developed a new open control architecture for the manipulator control. The control hardware is based on an industrial PC equipped with industrial data acquisition cards which read the manipulator joint positions and provide the actuator with the control actions through digital-to-analog converters. The software architecture is based on free and open source software: Orocos and ROS middleware. The proposed control architecture has two main advantages. First, the open control architecture allows us to eventually implement and program any required control algorithm by only plugging in the appropriate module. Second, the price of this control system remains below 2000\$.

The control of a rehabilitation task should be performed in task space. Thus, we presented the direct and inverse kinematic equations for the PM which are programmed into the control unit as a part of the passivity-based control scheme. The control algorithm is a point-to-point controller that uses an estimation of the robot's velocity and an integral action to cancel the gravitational term of the robot. Different results demonstrating the tracking accuracy of the proposed controller have been included, showing an accurate response in terms of position error. Finally, we have presented a step-by-step approach in a didactic way, which can serve as an interesting reference for others to follow on the mechatronics design of PMs.

Funding

The authors wish to thank the Plan Nacional de I + D, Comisión Interministerial de Ciencia y Tecnología (FEDER-CICYT) for the partial funding of this study under project DPI2013-44227-R. We also want to thank the Fondo Nacional de Ciencia, Tecnología e Innovación (FONACIT-Venezuela) for its financial support under the project No. 2013002165.

ORCID

Angel Valera  <http://orcid.org/0000-0001-6843-6394>

References

- Araujo-Gómez, P., Díaz-Rodríguez, M., Mata, V., Valera, A., Page, A. (2016). Design of a 3-UPS-RPU parallel robot for knee diagnosis and rehabilitation. In: *ROMANSY 21-Robot Design, Dynamics and Control*. Switzerland: Springer International Publishing, 303–310.
- Bruyninckx, H., Soetens, P., Issaris, P., Leuven, K. (2002). The Orocos Project. <http://www.orocos.org>.
- Cao, R., Gao, F., Zhang, Y., Pan, D., Chen, W. (2015). A new parameter design method of a 6 DoF parallel motion simulator for a given workspace. *Mechanics Based Design of Structures and Machines* 43(1):118. doi:10.1080/15397734.2014.904234. Accessed date: August 2nd, 2017.
- Carretero, J., Nahon, M., Podhorodeski, R. (2000). Workspace analysis and optimization of a novel 3 DoF parallel mechanism. *International Journal of Robotics and Automation* 15(4):1021–1026. doi:10.1115/1.533542
- Cazalilla, J., Vallés, M., Valera, A., Mata, V., Díaz-Rodríguez, M. (2016). Hybrid force/position control for a 3 DoF 1T2R parallel robot: Implementation, simulations and experiments. *Mechanics Based Design of Structures and Machines* 44(1):16. doi:10.1080/15397734.2015.1030679
- Chablat, D., Wenger, P. (2003). Architecture optimization of a 3 DoF translational parallel mechanism for machining applications, the orthoglide. *IEEE Transactions on Robotics and Automation* 19(3):403–410. doi:10.1109/tra.2003.810242
- Clavel, R. (1988). *A Fast Robot with Parallel Geometry*. Proc. Int. Symposium on Industrial Robots, Lausanne, Switzerland, 91–100.
- Díaz, I., Gil, J. J., Sánchez, E. (2011). Lower-limb robotic rehabilitation: Literature review and challenges. *Journal of Robotics* 2011:1–11. doi:10.1155/2011/759764

- Díaz-Rodríguez, M., Mata, V., Valera, Á., Page, Á. (2010). A methodology for dynamic parameters identification of 3-DOF parallel robots in terms of relevant parameters. *Mechanism and Machine Theory* 45(9):1337–1356. doi:10.1016/j.mechmachtheory.2010.04.007
- Escamilla, R. F., MacLeod, T. D., Wilk, K. E., Paulos, L., Andrews, J. R. (2012). Cruciate ligament loading during common knee rehabilitation exercises. *Proceedings of the Institution of Mechanical Engineers, Part H: Journal of Engineering in Medicine* 226(9):670–680. doi:10.1177/0954411912451839
- Gan, D., Dai, J. S., Dias, J., Umer, R., Seneviratne, L. (2015). Singularity-free workspace aimed optimal design of a 2T2R parallel mechanism for automated fiber placement. *Journal of Mechanisms and Robotics* 7(4):041022. doi:10.1115/1.4029957
- Garage, W. (2009). Robot Operating System. www.ros.org. Accessed date: August 2nd, 2017.
- Girone, M., Burdea, G., Bouzid, M., Popescu, V., Deutsch, J. E. (2001). A Stewart platform-based system for ankle telerehabilitation. *Autonomous Robots* 10(2):203–212.
- Gough, V., Whitehall, S. (1962). *Universal Tyre Test Machine*. Proceedings 9th Int. Technical Congress FISITA, London, vol. 117, 117–135.
- Jamwal, P. K., Hussain, S., Xie, S. Q. (2015). Review on design and control aspects of ankle rehabilitation robots. *Disability and Rehabilitation: Assistive Technology* 10(2):93–101. doi:10.3109/17483107.2013.866986
- Lee, K. M., Arjunan, S. (1992). A three degrees of freedom micro-motion in-parallel actuated manipulator. In: Tzou, H. S., Fukuda, T., eds. *Precision Sensors, Actuators and Systems*. Dordrecht (Netherlands): Springer Science+Business Media B.V., 345–374.
- Li, Y., Xu, Q. (2007). Design and development of a medical parallel robot for cardiopulmonary resuscitation. *IEEE/ASME Transactions on Mechatronics* 12(3):265–273. doi:10.1109/tmech.2007.897257
- Merlet, J. P. (2006). *Parallel Robots*. Dordrecht (Netherlands): Springer Science & Business Media, B.V., 128.
- Mohan, S., Mohanta, J. K., Kurtenbach, S., Paris, J., Corves, B., Huesing, M. (2017). Design, development and control of a 2PRP-2PPR planar parallel manipulator for lower limb rehabilitation therapies. *Mechanism and Machine Theory* 112:272–294.
- Ortega, R., Perez, J. A. L., Nicklasson, P. J., Sira-Ramirez, H. (2013). *Passivity-Based Control of Euler-Lagrange Systems: Mechanical, Electrical and Electromechanical Applications*. Springer Science & Business Media.
- Ortega, R., Spong, M. W. (1989). Adaptive motion control of rigid robots: A tutorial. *Automatica* 25(6):877–888. doi:10.1016/0005-1098(89)90054-x
- Paul, R. P. (1981). *Robot Manipulators: Mathematics, Programming, and Control: The Computer Control of Robot Manipulators*. Cambridge, MA: MIT Press.
- Pierrot, F., Company, O. (1999). *H4: A New Family of 4 DoF Parallel Robots*. Proceedings of 1999 IEEE/ASME International Conference on Advanced Intelligent Mechatronics, Georgia, USA, 508–513.
- Ramsay, J. O., Silverman, B. W. (1997). *Functional Data Analysis*. Springer Series in Statistics. New York, NY: Springer.
- Rastegarpanah, A., Saadat, M., Borboni, A. (2016). Parallel robot for lower limb rehabilitation exercises. *Applied Bionics and Biomechanics* 2016:1–10. doi:10.1155/2016/8584735
- Stewart, D. (1965). A platform with six degrees of freedom. *Proceedings of the Institution of Mechanical Engineers* 180(1):371–386.
- Tsai, L. W. (1999). *Robot Analysis: The Mechanics of Serial and Parallel Manipulators*. New York, USA: John Wiley & Sons, INC.
- Vallés, M., Casalilla, J., Valera, A., Mata, V., Page, A., Díaz-Rodríguez, M. (2015). A 3PRS parallel manipulator for ankle rehabilitation: Towards a low-cost robotic rehabilitation. *Robotica*:1–19. doi:10.1017/s0263574715000120.
- Vallés, M., Díaz-Rodríguez, M., Valera, A., Mata, V., Page, A. (2012). Mechatronic development and dynamic control of a 3 DoF parallel manipulator. *Mechanics Based Design of Structures and Machines* 40(4):434–452. doi:10.1080/15397734.2012.687292
- Xu, W. L., Pap, J. S., Bronlund, J. (2008). Design of a biologically inspired parallel robot for foods chewing. *IEEE Transactions on Industrial Electronics* 55(2):832–841. doi:10.1109/tie.2007.909067
- Yoon, J., Ryu, J., Lim, K. B. (2006). Reconfigurable ankle rehabilitation robot for various exercises. *Journal of Robotic Systems* 22(S1):S15–S33. doi:10.1002/rob.20150
- Zarkandi, S. (2011). Kinematics and singularity analysis of a parallel manipulator with three rotational and one translational DOFs. *Mechanics Based Design of Structures and Machines* 39(3):392–407. doi:10.1080/15397734.2011.559149